ACADEMIC PRESS

Available online at www.sciencedirect.com

SCIENCE DIRECT®

Journal of Sound and Vibration 267 (2003) 497–507

JOURNAL OF SOUND AND VIBRATION

www.elsevier.com/locate/jsvi

Squeal noise of rail-bound vehicles influenced by lateral contact position

F.G. de Beer*, M.H.A. Janssens, P.P. Kooijman

TNO-TPD, Stieltjesweg 1, P.O. Box 155, 2600 AD Delft, The Netherlands

Accepted 9 May 2003

Abstract

A frequency domain model has been developed to describe squeal noise of rail-bound vehicles generated by unstable lateral creepage between wheel and rail. The model is based on a combination of existing models for contact mechanics, contact dynamics, wheel dynamics and rail dynamics, which are transformed into the frequency domain. The relation between friction coefficient and lateral creepage is linearized to allow frequency domain calculations. This enables fast calculations and enhances insight into frequency-dependent phenomena relating to squeal. In addition to existing models, the variation of the normal contact force is implemented in the model. This addition to the model is essential to explain several effects. One of these effects is the influence of the lateral contact position on the wheel tread on squeal noise; squeal noise by lateral creepage only occurs for a certain contact position interval.

A laboratory test rig (scale 1:3) was designed to validate the model. Two measurements will be presented in this paper. The friction coefficient of the rolling contact is measured as a function of lateral creepage, for cases with and without squeal (but with the similar contact surface conditions), giving different results. The required wheel damping to prevent squeal noise is measured as a function of the lateral contact position. The test rig has been used for model validation and will be used to evaluate and optimize particular measures against squeal noise. The model can be used as a design tool for measures against squeal noise by lateral creepage.

1. Introduction

Curve squeal is the intense tonal noise that can occur when a railway vehicle traverses a curve or switch. Several mechanisms may generate squeal noise. During the curve passage, some wheels rub with the flange against the rail, causing noise. Other wheels (e.g., leading inner wheel of a bogie) perform lateral creepage because the wheel movement does not align with the rolling

*Corresponding author. Tel.: +31-15-269-2398; fax: +31-15-269-2111.
E-mail address: fdebeer@tpd.tno.nl (F.G. de Beer).

0022-460X/$ - see front matter
doi:10.1016/S0022-460X(03)00710-7

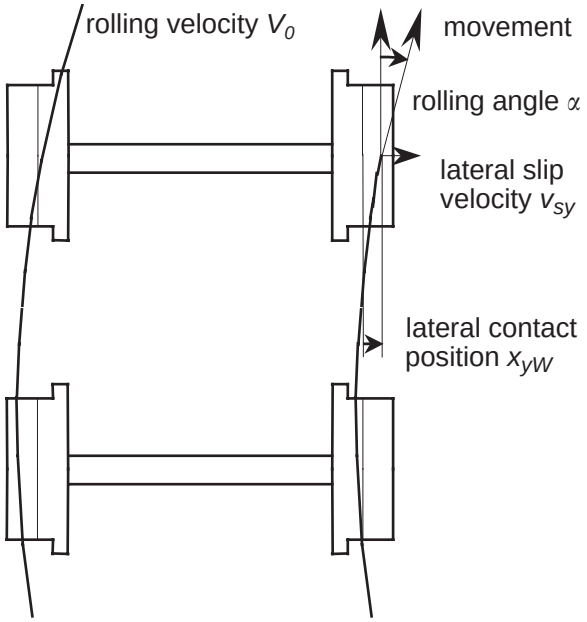

Fig. 1. Lateral contact position and creepage (creepage equals tan(α), with α being the rolling angle between rolling direction and direction of movement) of leading inner wheel.

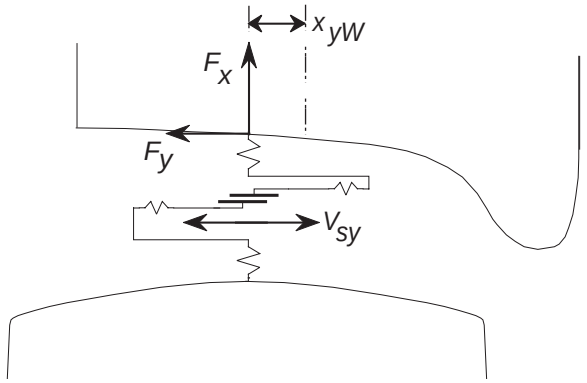

Fig. 2. Wheel and rail dynamics, friction element and contact springs model the complete system.

direction (Fig. 1). The creepage can show unstable stick–slip behaviour, causing the wheel to oscillate and radiate loud annoying noise. This article deals with squeal noise by this unstable lateral creepage.

This article describes a frequency domain model to predict the occurrence of squeal noise and the dominant frequency. The calculation and measurements of the amplitudes of the fundamental harmonic and higher harmonic components in sound pressure, contact forces and vibration velocities are described in Refs. [1–3].

The model for unstable lateral creepage is divided into several elements (see Fig. 2). These are: the friction element with the characteristics of the contact mechanics of the rolling contact

(Section 2); the dynamics of the contact area; the wheel and the rail (Section 3); and the Nyquist criterion for stability of the complete system (Section 4). With the help of this model, the influence of the lateral contact position is described in Section 5. A test rig (Section 6) was constructed for validation measurements of the friction coefficient and the influence of the lateral contact position (Section 7).

2. Contact mechanics

During a curve passage, the direction of movement and the rolling direction do not align, causing lateral creepage. Lateral creepage s is defined as the ratio of lateral creep velocity v_{sy} over the rolling velocity V_0, equal to $\tan(\alpha)$, with α being the rolling angle. The lateral creepage causes lateral contact force which equals the product of normal contact force and friction coefficient. Fingberg [4] gives equations for the stationary friction coefficient μ_0 of the non-rolling contact:

$$\mu_0 = \frac{\tau_R \tau_W}{(\tau_R + \tau_W)} \frac{\pi ab}{F_0}, \tag{1}$$

where τ_W, τ_R are the shear strength of the wheel and rail material (e.g., $4 \times 10^8 - 6 \times 10^8\,\mathrm{N/m^2}$), and a, b are the semi-axis length of the Hertz contact ellipse in the rolling and lateral direction (m), and for the creepage-dependent friction coefficient $\mu(s)$ of the rolling contact:

$$\begin{aligned}
&\mu(s) = -\mu_0\{s' - \tfrac{1}{3}s'^2 + \tfrac{1}{27}s'^3\}\{1 - 0.5\mathrm{e}^{-0.138/|sV_0|} - 0.5\mathrm{e}^{-6.9/|sV_0|}\} \quad \text{for } s' \leqslant 3,\\
&\mu(s) = -\mu_0\{1 - 0.5\mathrm{e}^{-0.138/|sV_0|} - 0.5\mathrm{e}^{-6.9/|sV_0|}\} \quad \text{for } s' > 3\\
&\quad \text{with } s' = \frac{sGabC_{22}}{\mu_0 F_0},
\end{aligned} \tag{2}$$

where G is the Shear modulus of steel and C_{22} the Kalkar constant ($C_{22} \approx 2.39 + 1.36(a/b) - 0.025(a/b)^2$)

For squealing wheels, the vertical contact force $F_0 + f_x(t)$, the lateral contact force $F_0\mu(s_0) + f_y(t)$, and the lateral slip $s_0 + v_{sy}(t)/V_0$ consist of a constant and a time-variant part. Their relation is

$$F_0\mu(s_0) + f_y(t) = (F_0 + f_x(t))\mu\left(s_0 + \frac{v_{sy}(t)}{V_0}\right). \tag{3}$$

If the situation for the onset of squeal is considered, in which the vibration amplitude is still very small, the non-linear friction coefficient $\mu(s)$ can be linearized and Eq. (3) becomes

$$F_0\mu(s_0) + f_y(t) \approx F_0\mu(s_0) + f_x(t)\mu(s_0) + \frac{F_0}{V_0}\frac{\partial\mu(s_0)}{\partial s} v_{sy}(t). \tag{4}$$

Transformation of the time-variant part from the time domain to the frequency domain gives

$$F_y(\omega) = F_x(\omega)\mu(s_0) + \frac{F_0}{V_0}\frac{\partial\mu(s_0)}{\partial s} V_{sy}(\omega). \tag{5}$$

This equation gives the lateral force as a result of vertical force and creepage following the characteristics of the friction element. In turn, the vertical force and the creep velocity are a function of the lateral force as described in the next section.

3. Wheel and rail dynamics

The TWINS software package [5] is used to calculate the wheel, rail and contact spring mobilities: Y_{Wxx}, Y_{Wyy}, Y_{Wyx} are the vertical, lateral and cross-mobility for the wheel in the contact point, Y_{Rxx}, Y_{Ryy}, Y_{Ryx} the vertical, lateral and cross-mobility for the rail in the contact point, and Y_{Cx}, Y_{Cy} the vertical and lateral mobility of the contact spring.

The relations for the vertical and lateral velocity over the friction element (see Fig. 2) are:

$$(F_x Y_{Wxx} + F_y Y_{Wyx}) + (F_x Y_{Cx}) + (F_x Y_{Rxx} + F_y Y_{Ryx}) = 0, \tag{6}$$

$$(F_x Y_{Wyx} + F_y Y_{Wyy}) + (F_y Y_{Cy}) + (F_x Y_{Ryx} + F_y Y_{Ryy}) = V_{sy}. \tag{7}$$

The wheel mobilities Y_{Wxx} and Y_{Wyx} depend on the lateral offset of contact position on the wheel, x_{yW}:

$$Y_{Wyx} = Y_{Wyx0} + x_{yW} Y_{Wyz0}, \tag{8}$$

$$Y_{Wxx} = Y_{Wxx0} + 2x_{yW} Y_{Wxz0} + x_{yW}^2 Y_{Wzz0}, \tag{9}$$

where Y_{Wyx0}, Y_{Wyz0}, Y_{Wxx0}, Y_{Wxz0}, Y_{Wzz0} are cross-mobilities between vertical and lateral forces and moment about the z-axis in the nominal lateral contact position on the wheel tread.

Substitution of Eqs. (6)–(9) gives the transfer functions for $F_x(\omega)/F_y(\omega)$ and $V_{sy}(\omega)/F_y(\omega)$.

4. Nyquist criterion for stability

Combination of the equations for contact mechanics and wheel dynamics gives a loop gain for the lateral contact force (see Fig. 3):

$$F_y(\omega) = H(\omega)F_y(\omega) \approx \left\{ \frac{F_x(\omega)}{F_y(\omega)} \mu(s_0) + \frac{V_{sy}(\omega)}{F_y(\omega)} \frac{F_0}{V_0} \frac{\partial \mu(s_0)}{\partial s} \right\} F_y(\omega). \tag{10}$$

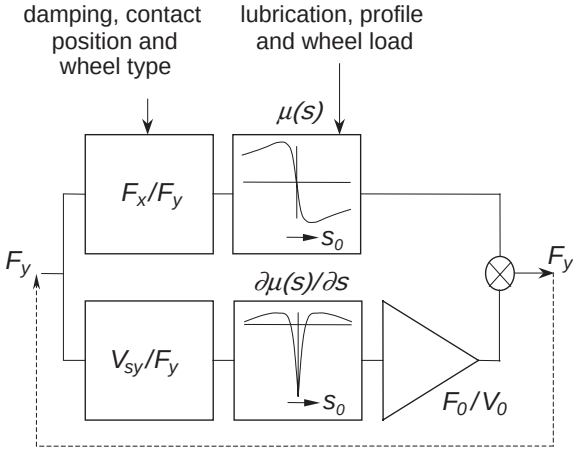

Fig 3. Schematic representation of influence of parameters on loop gain $H(\omega)$.

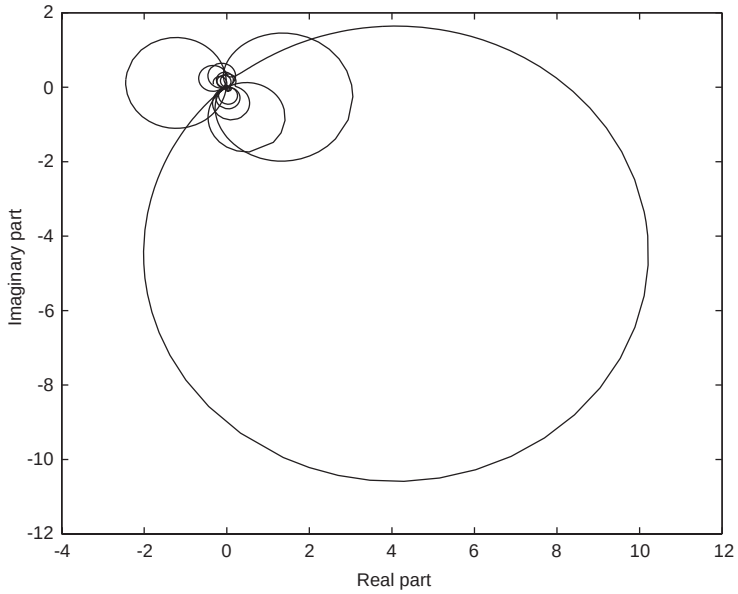

Fig. 4. Example of Nyquist contour $H(\omega)$ for test-rig wheel and $x_{yW} = 0.03\,\mathrm{m}$; several enclosures of point 1.

The instability of the system can be determined by the Nyquist criterion, which states that the system is unstable (the wheel squeals) for frequencies where the Nyquist contour $H(\omega)$ passes the real axis at the right-hand side of 1 (corresponding to a loop gain $H(\omega)$ larger than 1 and a phase shift of 0°) (see Fig. 4). The Nyquist contour (see Fig. 5) shows that squeal noise can occur at the frequencies of the axial wheel modes.

Heckl [6] shows that squeal noise occurs only at the resonance frequency of the mode with the largest growth factor. The growth factor is proportional to the ratio of the loop gain over the modal mass of the corresponding mode. The modal masses of the axial modes are approximately equal. Hence, the frequency of the mode with the largest loop gain becomes the dominant squeal-noise frequency ω_1. For the large variation in lateral creepage during squeal noise, the friction coefficient can no longer be linearized. The non-linear relationship between friction coefficient $\mu(s)$ and lateral creepage s causes higher harmonics in the force and vibration spectra. The lateral vibration of the wheel will therefore consist of the dominant frequency and higher harmonics, $k\omega_1$, with $k = 1, 2, 3, \ldots$ [3].

5. Contact position

Figs. 6 and 7 show the influence of the contact position on the transfer functions $V_{sy}(\omega_n)/F_y(\omega_n)$ and $F_x(\omega_n)/F_y(\omega_n)$ with ω_n equal to the axial wheel mode frequencies with 0 nodal circles and n nodal diameters. These figures show symmetry about the symmetry area of the wheel itself (the $x_{yW} = 0$ position). However, asymmetric wheels with a flange have asymmetric graphs for $F_x(\omega_n)/F_y(\omega_n)$ and $V_{sy}(\omega_n)/F_y(\omega_n)$ plotted against x_{yW}.

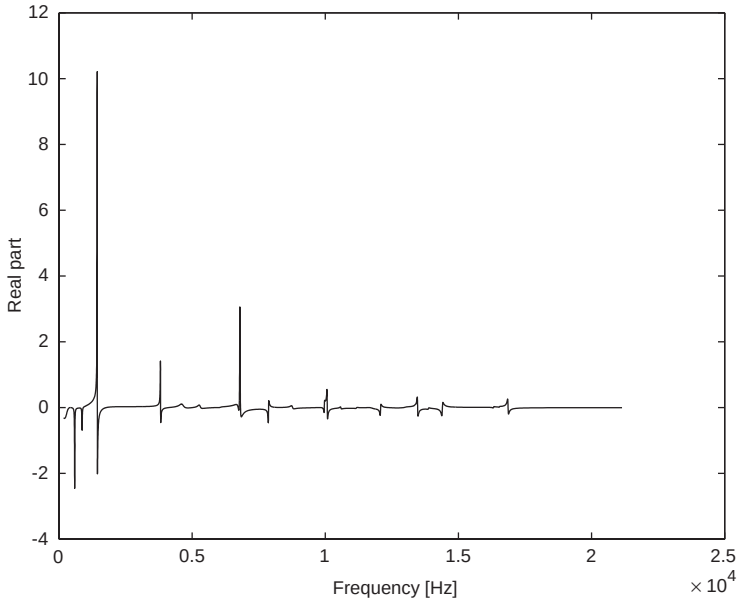

Fig. 5. Real part of Nyquist contour $H(\omega)$ for test-rig wheel and $x_{yW} = 0.03\,\mathrm{m}$; peak values at axial wheel mode frequencies.

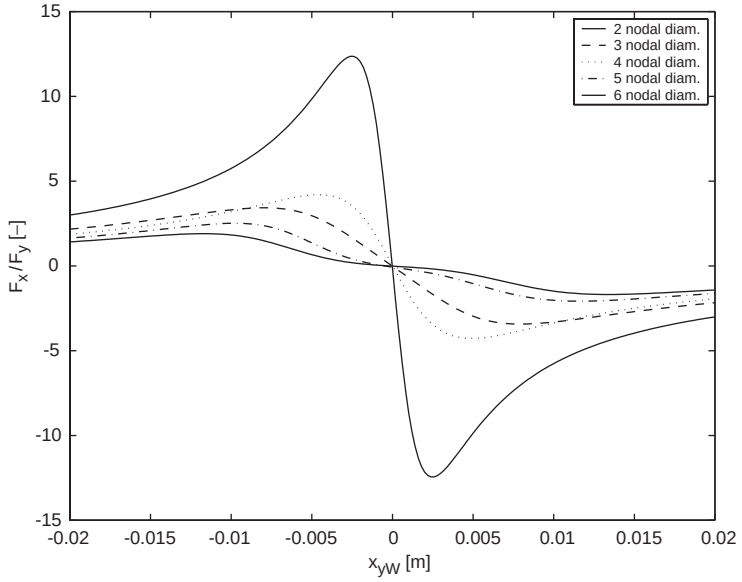

Fig. 6. Transfer function $\mathrm{Re}\{F_x/F_y\}$ for axial modes of test-rig wheel against contact position x_{yW}.

The contact position also influences the loop gain $H(\omega)$ (see Eq. (10)), via the transfer functions. For the test-rig wheel, the loop gain $\mathrm{Re}\{H(\omega)\}$ only exceeds 1 for $x_{yW}s_0 \gg 0$ (Fig. 8). Hence, the model predicts only instability and squeal noise for $x_{yW}s_0 \gg 0$.

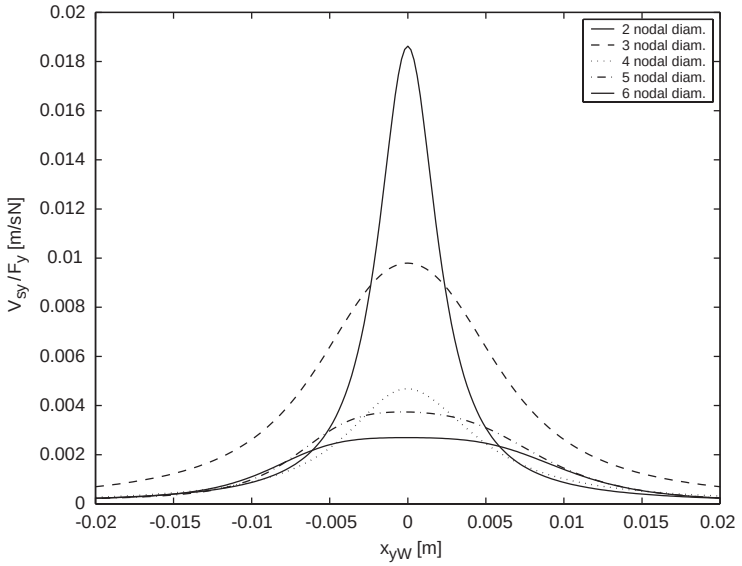

Fig. 7. Transfer function $\mathrm{Re}\{V_{sy}/F_y\}$ for axial modes of test-rig wheel against contact position x_{yW}.

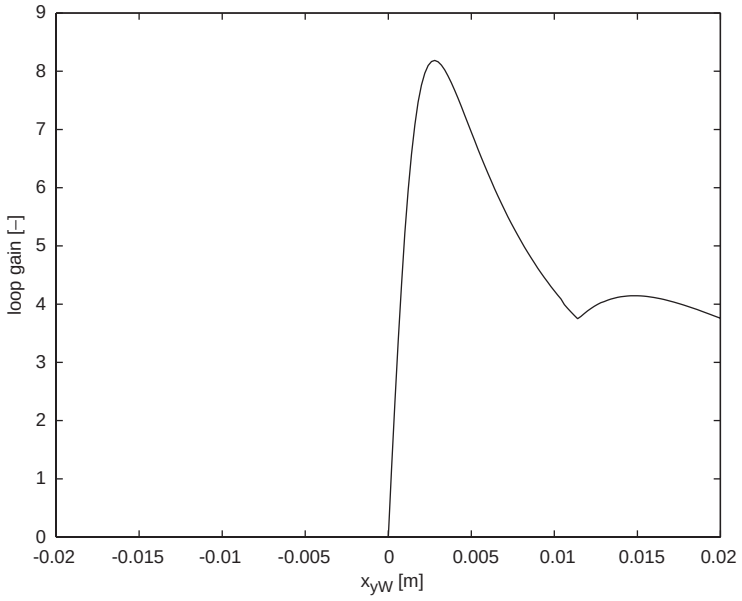

Fig. 8. Maximum loop gain for undamped wheel under test conditions ($s = 0.013$) against lateral contact position x_{yW}.

6. Test rig

The laboratory test rig is a scale model (1:3) of an undamped wheel running on a second damped wheel which represents the rail ('rail–wheel') (see Fig. 9). Several conceptual solutions have been considered but this concept has been chosen because it facilitated a test rig which is

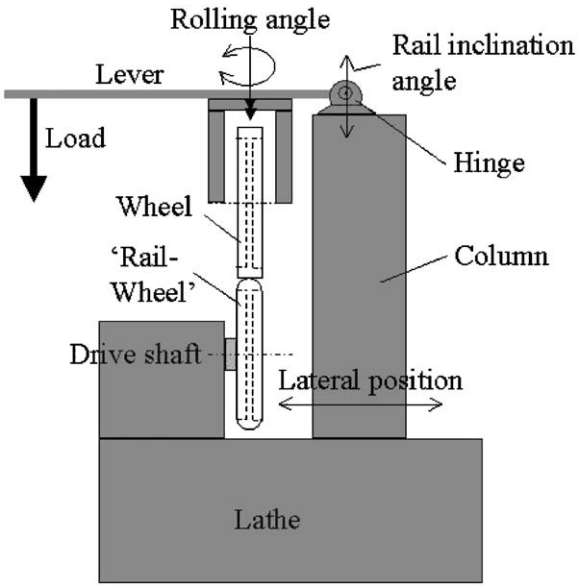

Fig. 9. Laboratory test rig for squeal-noise measurements with two 1:3-scale wheels built onto a lathe, which provides the drive at adjustable speeds.

compact and therefore easy to control and the contact point location is fixed and therefore contact forces and vibrations are easy to measure. The disadvantage of this concept is that the 'rail–wheel' has a finite radius of curvature in the tangential direction, whereas for an actual rail this radius is infinite. Adjusting the lateral radius of the rail compensates for the effect on the contact patch. In this way the various important contact parameters can be adjusted within approximately 10% of their value for an actual wheel/rail contact.

Ideally, the 'rail–wheel' dynamics should resemble the rail dynamics. From theory, however, it appears that this is not very critical as long as the rail receptance is much lower than the wheel receptance at the wheel resonance frequencies. This is realized by increasing the damping of the 'rail–wheel' by means of a pack of thin steel plates on both sides of the web. This damping method proved to be very effective ($\eta > 0.1$). Squeal noise in the wheel can be generated by an adjustable misalignment of the axes of both wheels, which results in a certain rolling angle. Other parameters that can be controlled and/or monitored in the test rig are: wheel dynamics (impedance) by interchanging wheels; wheel damping by gradually adding damping plates (as used for the rail–wheel); lateral position of the contact patch on the wheel; rolling speed; rail inclination angle; axle load; transverse radii of wheel and rail (by interchanging wheels); the surface conditions of wheel and rail–wheel; temperature and humidity. These parameters are relevant for squeal noise and cover all parameters that occur in practice.

7. Measurement results

The friction coefficient depends on various parameters, e.g., the contact geometry, surface conditions, pre-load and, most importantly, on rolling angle. The friction coefficient can be

estimated using Eqs. (1) and (2) or measured using the test rig. By definition, the friction coefficient is the ratio of the lateral over the vertical contact force. Fig. 10 presents the friction coefficient as a function of the rolling angle for cases with and without squeal noise, with similar conditions other than the changing contact position. Below a rolling angle of 0.4°, squeal does not occur and the results of both measurements are the same. Above 0.4°, squeal noise occurs and the lateral creepage oscillates with large amplitude. As a consequence, the friction coefficient also oscillates with an average value below the stationary value of the non-squealing situation (similar to Remington [7]). Note that the friction coefficient is relatively high in these measurements and calculations due to a pre-load of 1 kN, which is relatively low for tram, metro or train operation.

Given various uncertainties, e.g., in τ_W, τ_R and surface conditions, the agreement between calculations and measurements for the non-squealing case is very good (see Figs. 10 and 11). For the squealing case the agreement is clearly less. Although the cut-on angle for squeal for both

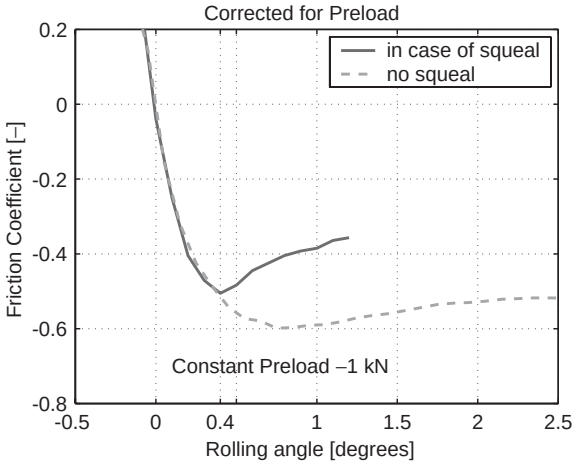

Fig. 10. Measured friction coefficient for stable and unstable creepage.

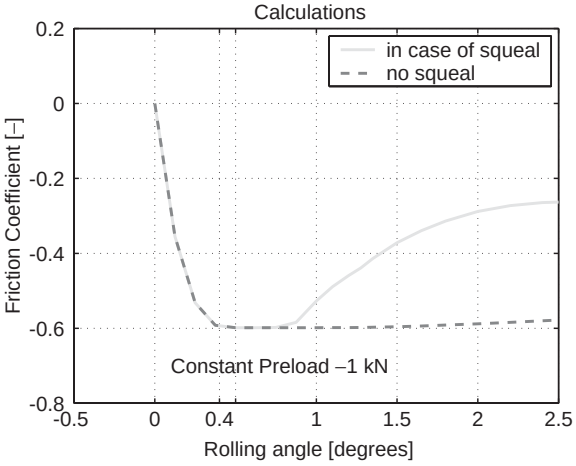

Fig. 11. Calculated friction coefficient for the test rig; $\tau_W = 530\,\mathrm{N/mm^2}$, $\tau_R = 530\,\mathrm{N/mm^2}$, $ab = 0.72\,\mathrm{mm^2}$, $F_0 = 1\,\mathrm{kN}$.

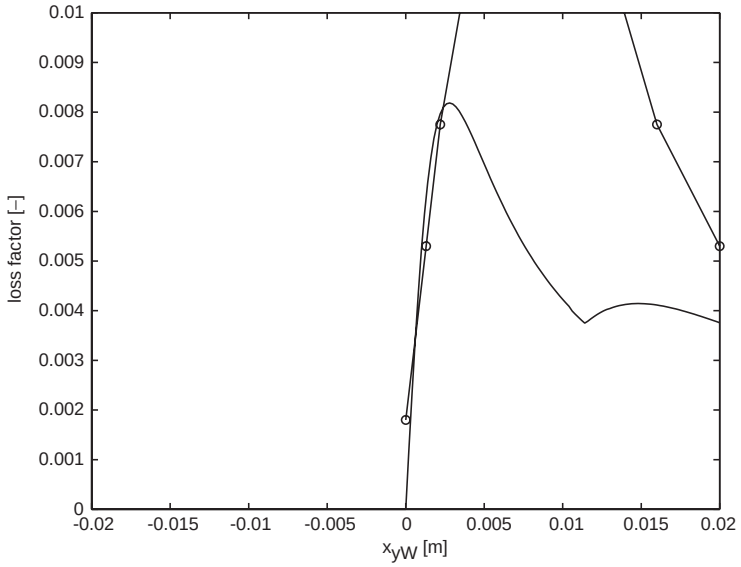

Fig. 12. Minimal required loss factor for wheel under test conditions ((o—o) measured and (—) calculated). Wheel squeal occurred in range $0.003 < x_{yW} < 0.014$ because a loss factor above 0.01 could not be achieved with thin steel plates.

calculations and measurements is about 0.4° here, the drop of the friction coefficient observed in the measurements is hardly visible in the calculation for the range from 0.4° to 0.8° (although present).

The influence of the lateral contact position on the occurrence of squeal noise is verified by measuring the minimum required loss factor of the wheel to prevent squeal noise. For a given contact position, x_{yW}, and fixed rolling angle ($\alpha = 0.75°$ or $s_0 = 0.013$), wheel damping is increased by mounting thin steel plates to the wheel until squeal noise stopped. For this situation, the loss factor was measured. Fig. 12 shows that squeal noise does not occur for negative contact positions. For positive positions, the required damping depends on the position. Measurement and calculated results are again in reasonable agreement, given the above-mentioned uncertainties.

8. Conclusions

Based on existing models for contact mechanics, contact dynamics, wheel dynamics and rail dynamics, a frequency domain model has been developed for squeal noise generated by lateral creepage. An essential step in the transformation from time to frequency domain is the linearization of the friction coefficient, which is allowed for small vibration amplitudes at the onset of squeal noise. The next step is to use the Nyquist criterion to determine whether or not squeal noise occurs and at which frequency. The model has a short calculation time and an insight into related frequency-dependent phenomena. The model predicts squeal noise for any given wheel, rail, wheel load, lateral contact position on wheel tread, rolling velocity and rolling angle. The model is validated and used as a design tool for measures against squeal noise.

In practice, the wheel receptance exceeds the rail receptance at wheel resonance frequencies. Therefore, the wheel dynamics play a significant role in squeal noise while the rail dynamics can initially be neglected. Squeal by lateral creepage occurs at one of the resonance frequencies of axial wheel modes. The lateral contact position on the wheel tyre influences the occurrence of squeal noise and which resonance frequency becomes dominant.

A laboratory test rig was designed for rail-bound vehicle squeal-noise research. This test rig comprises a 1:3-scale model of a wheel. Using the test rig, squeal noise by lateral creepage can be generated and measurements can be performed in a well-controlled environment. This allows the acquisition of data [2,3] that can be used for validation of the theoretical model. Furthermore, the test facility can be used to evaluate and optimize particular measures against squeal noise such as wheel damping, lubrication, wheel and/or rail transverse profile adjustment.

The friction coefficient of the rolling contact was measured as a function of the rolling angle. This was done for a situation in which squeal noise occurs and in a situation without squeal noise (but with similar contact surface conditions such as no lubricants, etc.). For the non-squealing case agreement between experiment and calculations was good. For the squealing case, it is expected from theory that the friction coefficient diminishes. This was confirmed in the measurement, although the effect was much greater than indicated by the calculations. This is a topic for further research.

Measurements were performed for fixed lateral creepage, s_0, and a varying contact position on the wheel tread, x_{yW}. The results show that squeal noise only occurs for $x_{yW}s_0 \gg 0$. This means that for the leading inner wheel of a bogie, squeal noise only occurs for a contact position on the outside of the wheel tread (opposite to the flange).

The influence of the contact position on squeal noise by lateral creepage can be used to design a measure against squeal noise. For example, by adjusting the rail profile, the contact position on the wheel tread can be shifted and squeal noise can be prevented. The influence of the contact position can also be an explanation for the effect that two apparently equal curves show a different squeal-noise behaviour for the same vehicles at the same velocity.

References

[1] F.G. de Beer, M.H.A. Janssens, P.P. Kooijman, W.J, van Vliet, Curve squeal of rail bound vehicles, Part 1: frequency domain calculation model, *Proceedings of the Internoise 2000*, Nice, France, 2000.

[2] P.P. Kooijman, M.H.A. Janssens, W.J, van Vliet, F.G. de Beer, Curve squeal of rail bound vehicles, Part 2: set-up for measurement of creepage dependent friction coefficient, *Proceedings of the Internoise 2000*, Nice, France, 2000.

[3] M.H.A. Janssens, W.J, van Vliet, P.P. Kooijman, F.G. de Beer, Curve squeal of rail bound vehicles, Part 3: measurement techniques for wheel/rail contact velocities and forces at squeal noise frequencies, *Proceedings of the Internoise 2000*, Nice, France, 2000.

[4] U. Fingberg, A model of wheel–rail squealing noise, *Journal of Sound and Vibration* 143 (1990) 365–377.

[5] D.J. Thompson, M.H.A. Janssens, F.G. de Beer, Theoretical manual, TWINS version 3.0, TNO-report TPD-HAG-990211, TNO Institute of Applied Physics, 1999.

[6] M.A. Heckl, Curve squeal of train wheels, Part 2: which wheel modes are prone to squeal? *Journal of Sound and Vibration* 229(3) (2000) 695–707.

[7] P.J. Remingtion, Wheel/rail squeal and impact noise: what do we know? What don't we know? Where do we go from here? *Journal of Sound and Vibration* 116(2) (1985) 339–353.